

Role of second-order optical potential in pion-oxygen scattering

L.C. Liu and C.M. Shakin

Institute of Nuclear Theory and Department of Physics, Brooklyn College of the City University of New York, Brooklyn, New York 11210

(Received 7 March 1978)

We analyze π - ^{16}O elastic scattering at pion energies between 40 and 340 MeV. An excellent fit to the data follows from the inclusion of a second-order optical potential. The parameters specifying the second-order potential are found to exhibit marked resonance behavior. The magnitude and the energy dependence of the parameters of the second-order potential obtained for pion-oxygen scattering are, in the main, very similar to that determined for pion-carbon scattering. This result indicates that a universal parametrization of the second-order pion-nucleus optical potential may be possible.

[NUCLEAR REACTIONS Pion-oxygen scattering at 40, 49.7, 50, 79.3, 114.3, 162.6, 240.2, and 342.6 MeV. Parameters of second-order optical potential.]

I. INTRODUCTION

In recent years extensive calculations have been made of the first-order pion-nucleus optical potential. It has been found that a careful treatment of the binding and Fermi motion of the target nucleons is needed to obtain a good representation of the data.¹ [It is worth noting that our treatment of Fermi motion is quite different from the so-called "Fermi averaging" introduced in the context of the fixed-scatterer approximation (FSA).²] To some extent, however, the results of a complete treatment of Fermi motion and binding can be simulated by introducing a phenomenological energy shift parameter in the π - N T matrix in an FSA calculation.³ We do not require such an energy shift in our work since we do not make use of the FSA.

We believe that our parameter-free calculation of the first-order optical potential is quite accurate. We are therefore in a position to study the second-order optical potential and to introduce phenomenological parameters only in the specification of that potential. In an earlier work, we have studied the second-order potential in the case of pion-carbon scattering.⁴ In this work we extend the analysis to the study of pion-oxygen scattering. As we will see, the second-order potential determined for pion-oxygen scattering is similar to that found for pion-carbon scattering over a large energy range. {Reference 4 also contains a similar analysis for π - ^4He scattering, however, the parameters of the second-order potential obtained from the analysis of π - ^4He are different than those obtained for π - ^{12}C and π - ^{16}O scattering. We believe this is due to the fact that ^4He has very few particles and, while the form used for the second-order potential [Eq.

(2.1)] may allow for a universal parametrization for ^{12}C , ^{16}O , and possibly heavier nuclei, its use in the case of very light nuclei such as ^4He seems to require a modified parametrization. For these reasons, we do not discuss the ^4He parametrization in this work.}

II. DISCUSSION AND RESULTS

Our optical potential may be written as

$$\langle \vec{k}' | V^{(1)}(\sqrt{s}) | \vec{k} \rangle + \langle \vec{k}' | V^{(2)}(\sqrt{s}) | \vec{k} \rangle.$$

The first-order potential, $V^{(1)}$, has been discussed extensively in earlier publications.⁵ The second-order potential, introduced previously,^{1,4} may be written

$$\langle \vec{k}' | V^{(2)}(\sqrt{s}) | \vec{k} \rangle = R^{1/2}(\vec{k}') (2M_A) \bar{G}(\vec{k} - \vec{k}') A(A-1) \times [B(\sqrt{s}) + C(\sqrt{s}) \vec{k}' \cdot \vec{k}] R^{1/2}(\vec{k}), \quad (2.1)$$

where $\sqrt{s} = (\vec{k}_0^2 + M_\pi^2)^{1/2} + (\vec{k}_0^2 + M_A^2)^{1/2}$. Here \vec{k}_0 is the momentum of the pion in the c.m. frame of the pion-nucleus system and $R^{1/2}(\vec{k})$ is a kinematical factor defined in Ref. 4. Further,

$$\bar{G}(\vec{k} - \vec{k}') \equiv (2\pi)^3 \int e^{i(\vec{k} - \vec{k}') \cdot \vec{r}} \rho^2(\vec{r}) d\vec{r}, \quad (2.2)$$

where $\rho(\vec{r})$ is the nuclear matter density.

In the literature, a coordinate-space phenomenological second-order potential of the form

$$\langle \vec{r}' | U^{(2)} | \vec{r} \rangle \sim \delta(\vec{r}' - \vec{r}) [B(\sqrt{s}) \rho^2(\vec{r}) + C(\sqrt{s}) \vec{\nabla} \cdot \rho^2(\vec{r}) \vec{\nabla}] \quad (2.3)$$

is widely employed to represent absorption effects in the study of π -nucleus scattering and π -mesic atoms. This is a local potential and is a reasonable form if the range of interaction can be considered small in comparison to the size of nucleus. The Fourier transform of Eq. (2.3) is giv-

en by

$$\langle \vec{k}' | U^{(2)} | \vec{k} \rangle \sim [B(\sqrt{s}) + C(\sqrt{s}) \vec{k}' \cdot \vec{k}] \bar{G}(\vec{k} - \vec{k}'). \quad (2.4)$$

Except for a kinematical factor $R^{1/2}(\vec{k}')R^{1/2}(\vec{k})$, Eq. (2.4) is identical to $V^{(2)}$ defined in Eq. (2.1). In the calculation of the first-order potential, the factors $R^{1/2}(\vec{k})$ and $R^{1/2}(\vec{k}')$ arose when making the reduction from the four-dimensional formalism to the (covariant) three-dimensional formalism. Such factors would also arise in reducing the covariant second-order potential to the form appropriate for the three-dimensional formalism. However, at this stage of development one may just as well interpret $V^{(2)}$ of Eq. (2.1) as the potential $U^{(2)}$ of Eqs. (2.3) and (2.4) supplemented by a product of "form factors," $R^{1/2}(\vec{k})R^{1/2}(\vec{k}')$. (Form factors have also been introduced by Landau and Thomas⁹ in the specification of a momentum-space optical potential which describes pion absorption. The form for this potential chosen by these authors is essentially the same as the form we have used.)

In Eq. (2.1), $B(\sqrt{s})$ and $C(\sqrt{s})$ are complex numbers. Therefore, we have four real parameters at each energy. We present the results of calculations for pion-oxygen scattering from 40 MeV to 340 MeV (Refs. 6, 7) in Figs. 1-3. The dashed

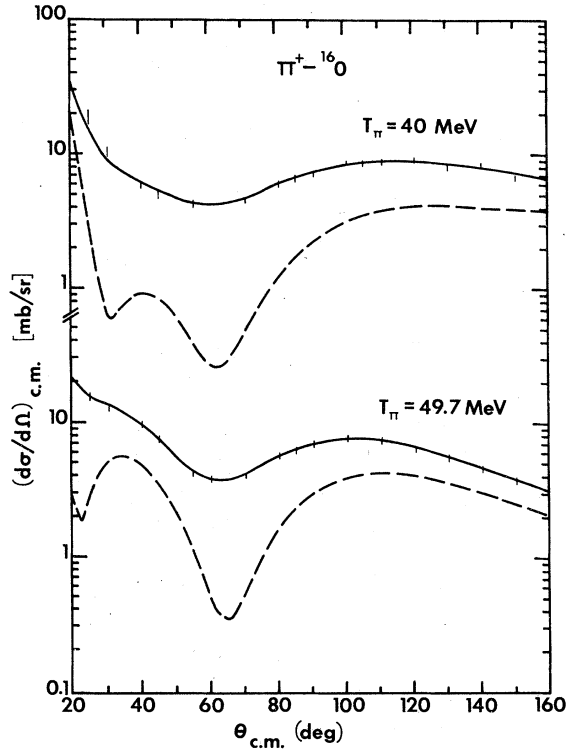


FIG. 1. The differential cross sections for $\pi^+{}^{16}\text{O}$ scattering at 40 and 49.7 MeV. The data are from Ref. 5. The dashed line shows the result of using $V^{(1)}$ only while the inclusion of $V^{(2)}$ yields the solid line. (See Table I.)

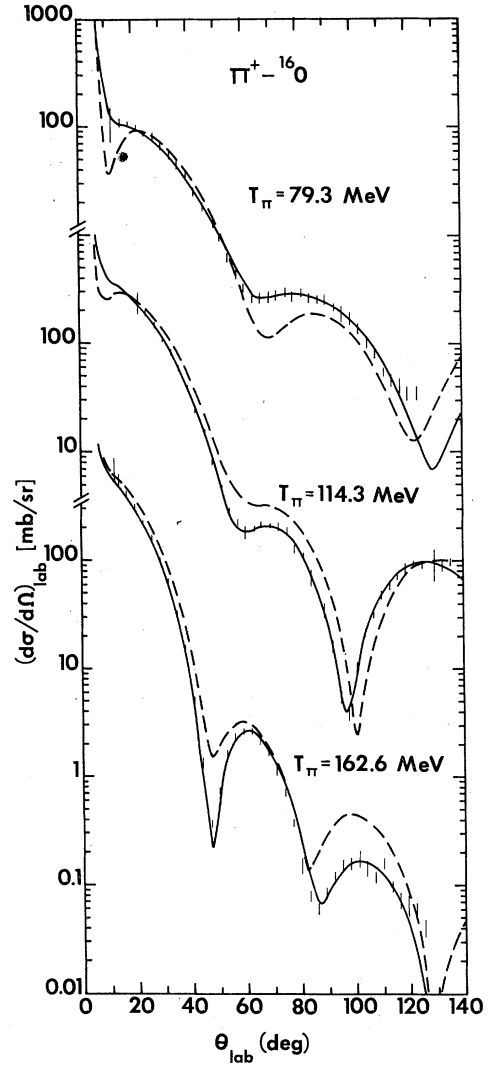


FIG. 2. The differential cross sections for $\pi^+{}^{16}\text{O}$ scattering at 79.5, 114.3, and 162.6 MeV. The data are taken from Ref. 6. Calculations of $\pi^+{}^{16}\text{O}$ scattering at 114.3 and 162.6 MeV yield fits of similar quality. The parameters of $V^{(2)}$ are given in Table I.

curves represent the result for $V^{(1)}$ only, i.e., $B=C=0$. The solid curves are obtained with the values of B and C listed in Table I. The values of $(B+k_0^2C)$ are also given in Table I. (The errors in the parameters listed in this table are representative of the range of variation of the parameters that does not lead to an appreciable increase of the χ^2 value.)

In Fig. 4 we present $\text{Im}(B+k_0^2C)$ and in Fig. 5 we present $\text{Re}(B+k_0^2C)$. In Figs. 4 and 5 we also show the values of $|\text{Im}(B+k_0^2C)|$ and $\text{Re}(B+k_0^2C)$ obtained in our previous analysis of pion-carbon scattering.⁴ In the resonance region the parameter B is small compared to k_0^2C and the general agreement for the parameters for carbon and

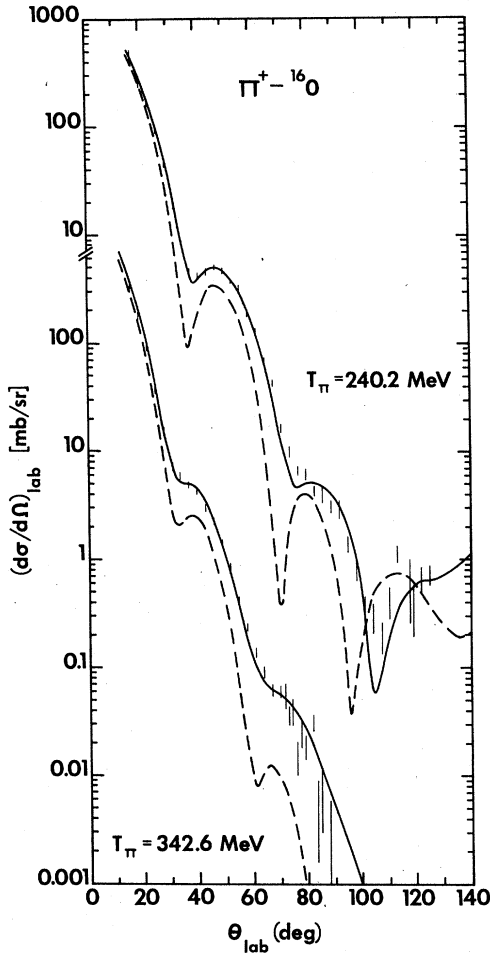


FIG. 3. The differential cross section for $\pi^+ - {}^{16}\text{O}$ scattering at 240 and 342.6 MeV. The data are taken from Ref. 6 (See Table I.)

oxygen seen in Figs. 4 and 5 reflects the similarity of the values of $k_0^2 C$ for the two targets. This indicates that it may be possible to obtain a universal parametrization of the part of the second-order potential proportional to $C(\sqrt{s})$. (The values for B and $k_0^2 C$ obtained from the analysis of $\pi - {}^{12}\text{C}$ scattering may be found in Ref. 4.)

A systematic comparison of the values of $\text{Re}B$, $\text{Im}B$, $\text{Re}(k_0^2 C)$, and $\text{Im}(k_0^2 C)$ for ${}^{12}\text{C}$ and ${}^{16}\text{O}$ shows generally good agreement in the values of $\text{Re}(k_0^2 C)$ and $\text{Im}(k_0^2 C)$. The worst case seems to be for $\text{Im}(k_0^2 C)$ for π^- scattering at 150, 163, and 180 MeV. Here the lack of agreement between the ${}^{12}\text{C}$ and ${}^{16}\text{O}$ parameters is of the order of twenty percent. Otherwise the agreement is good, considering the large range of variation of $\text{Re}(k_0^2 C)$ and $\text{Im}(k_0^2 C)$. Except for a point at 28 MeV (for ${}^{12}\text{C}$), the values of $\text{Im}B$ are very small for both ${}^{16}\text{O}$ and ${}^{12}\text{C}$ and little modification of the fit to the data will follow if these parameters are put equal to

zero.

The situation in the case of $\text{Re}B$ is less satisfactory since these parameters exhibit rather scattered values in the energy region 100–170 MeV. However, we do not have measurements for ${}^{16}\text{O}$ and ${}^{12}\text{C}$ at the same energies in this region. It is possible that further measurements and additional phenomenological fits will clarify the behavior of the parameter $\text{Re}B$.

In Table II we present values of the phase shifts and inelasticity parameters obtained using $V^{(1)}$ alone [columns (a)] and also those values obtained with $V^{(1)} + V^{(2)}$ [columns (b)]. The contributions to the reaction cross sections for each partial wave are also given in the table. [Note that $\sigma_{r,i} = 4\pi \times (2l+1)(1-\eta_i^2)/4k_0^2$.] It may be seen from this table that the inclusion of the second-order potential leads to a large increase in the reaction cross section at the lower energies, while the reaction cross sections at 240 MeV exhibit only small changes. It may also be seen that in many cases the values of η_i are quite small, yielding reaction cross sections close to the unitary limit. For example, at 240 MeV, the imaginary part of $V^{(1)}$ is very large, leading to small values of η_i . Therefore, the inclusion of $V^{(2)}$ leads to only small changes in the reaction cross sections at 240 MeV.

In Table III we present the values of two forward scattering amplitudes, $\mathcal{F}_N(0)$ and $f_N(0)$. The former is calculated without the Coulomb interaction. Again, column (a) denotes the result for $V^{(1)}$ only and column (b) contains the result for $V^{(1)} + V^{(2)}$. The amplitude f_N represents the difference between the total amplitude and the Coulomb amplitude and for $\theta=0$, is given by

$$f_N(0) = \sum_l (2l+1) e^{2i\sigma_l} (\eta_l e^{2i\sigma_l} - 1) / 2ik_0. \quad (2.5)$$

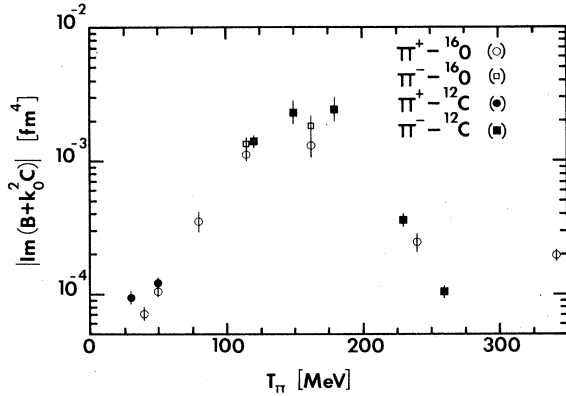
As may be seen from Table III, the inclusion of the second-order potential leads to significant changes in both $\mathcal{F}_N(0)$ and $f_N(0)$. At the lower energies there are important modifications in both the real and imaginary parts of these amplitudes. At the higher energies the main modification upon the inclusion of $V^{(2)}$ appears in $\text{Re}\mathcal{F}_N(0)$ calculated with and without $V^{(2)}$. [The amplitudes $\mathcal{F}_N(0)$ calculated in the absence of the Coulomb potential are of interest in the study of pion-nucleus scattering via dispersion relations.]

It is worth noting that the $\pi-N$ T matrices used to construct $V^{(1)}$ were taken from Ref. 8 (LMM). Since the LMM model specifies a single separable form in each $\pi-N$ channel, the low-energy P_{11} phase shifts have the wrong sign in this model. We have modified the LMM model to reproduce the correct on-shell values of the $\pi-N$ T matrix in the P_{11} channel. However, the subthreshold be-

TABLE I. Parameters of the second-order optical potential for pion-oxygen scattering.

T^{lab} (MeV)	$B(\sqrt{s})$ (10^{-4} fm)	$k_0^2 C(\sqrt{s})$ (10^{-4} fm)	$B(\sqrt{s}) + k_0^2 C(\sqrt{s})$ (10^{-4} fm)
40 (π^+)	(1.08 \pm 0.10)	(-0.87 \pm 0.28)	(0.2 \pm 0.4)
	$+i(-0.078 \pm 0.10)$	$+i(-0.72 \pm 0.06)$	$+i(-0.8 \pm 0.2)$
49.7 (π^+)	(0.97 \pm 0.05)	(-0.96 \pm 0.01)	(0.01 \pm 0.1)
	$+i(-0.038 \pm 0.001)$	$+i(-1.11 \pm 0.04)$	$+i(-1.15 \pm 0.04)$
79.3 (π^+)	$+i(-0.0145 \pm 0.0014)$	$+i(-1.07 \pm 0.04)$	$+i(-1.08 \pm 0.04)$
	(0.337 \pm 0.043)	(-0.595 \pm 0.050)	(-0.258 \pm 0.093)
114.3 (π^+)	$+i(-0.050 \pm 0.070)$	$+i(-3.64 \pm 0.57)$	$+i(-3.69 \pm 0.64)$
	(2.94 \pm 0.14)	(-6.58 \pm 0.33)	(-3.64 \pm 0.47)
162.6 (π^+)	$+i(-0.245 \pm 0.012)$	$+i(-11.3 \pm 0.40)$	$+i(-11.5 \pm 0.40)$
	(-2.75 \pm 0.45)	(7.33 \pm 0.35)	(4.58 \pm 0.80)
240.2 (π^+)	$+i(-0.359 \pm 0.170)$	$+i(-13.5 \pm 0.60)$	$+i(-13.8 \pm 0.70)$
	(0.329 \pm 0.004)	(21.9 \pm 2.0)	(22.2 \pm 2.0)
342.6 (π^+)	$+i(-0.607 \pm 0.300)$	$+i(-1.85 \pm 0.09)$	$+i(-2.45 \pm 0.39)$
	(3.97 \pm 0.30)	(3.73 \pm 0.30)	(7.70 \pm 0.60)
114.3 (π^-)	$+i(-1.99 \pm 0.05)$	$+i(-0.0147 \pm 0.0020)$	$+i(-2.00 \pm 0.05)$
	(3.21 \pm 0.16)	(-7.34 \pm 0.36)	(-4.13 \pm 0.52)
162.6 (π^-)	$+i(-0.0014 \pm 0.0014)$	$+i(-13.3 \pm 0.40)$	$+i(-13.3 \pm 0.40)$
	(-2.75 \pm 0.12)	(5.57 \pm 0.22)	(2.82 \pm 0.34)
	$+i(-0.0012 \pm 0.0012)$	$+i(-18.3 \pm 0.80)$	$+i(-18.3 \pm 0.80)$

havior of the π - N T matrix (in all channels) is not given correctly in that model. For example, the s and u channel nucleon poles of the physical π - N T matrix are absent in the LMM model. Because of these deficiencies, we feel that additional calculations at low energy (40–80 MeV) using an improved model¹⁰ of the off-shell π - N T matrix are necessary. Calculation of low-energy pion nucleus scattering using such an improved π - N T matrix and including a detailed treatment of Pauli principle corrections are underway. It is quite possible that at low energies, the first-order potential, $V^{(1)}$, resulting from such calculations may be quite different from the potential used in

FIG. 4. The values of $\text{Im}(B+k_0^2 C)$ determined from the study of π - ^{12}C and π - ^{16}O elastic scattering.

this work. Therefore we believe that the parameters $B(\sqrt{s})$ and $k_0^2 C(\sqrt{s})$ given in Table I for $T_\pi = 40$ and 49.7 MeV will be modified when we attempt to fit the data using our improved calculation of $V^{(1)}$.

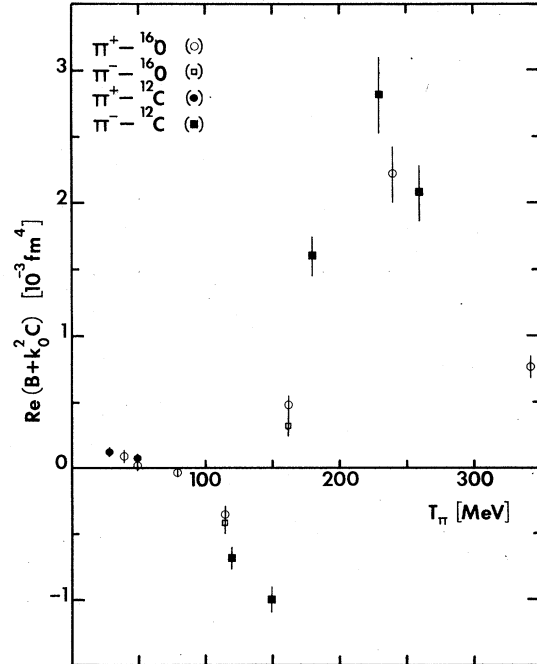
FIG. 5. The values of $\text{Re}(B+k_0^2 C)$ determined from the study of π - ^{12}C and π - ^{16}O elastic scattering.

TABLE II. Phase shifts, inelasticity parameters, and reaction cross sections for pion-oxygen scattering calculated: (a) without and (b) with the second-order potential.

T_{π^+} (MeV)	l	δ_l (degree)		η_l		σ_{rI} (mb)	
		(a)	(b)	(a)	(b)	(a)	(b)
40	0	-5.8	-15.4	0.96	0.94	8.6	11.1
	1	9.6	10.8	0.98	0.85	12.1	83.3
	2	3.6	4.2	0.996	0.96	4.4	37.5
79.3	3	0.44	0.5	1.0	0.997	0.44	3.6
	0	37.3	-11.0	0.52	0.34	32.0	39.0
	1	24.1	14.5	0.81	0.40	46.4	111
114.3	2	20.1	14.6	0.86	0.57	57.1	150
	3	6.2	5.6	0.96	0.89	22.1	64.8
	4	1.1	1.1	0.995	0.99	3.8	9.6
162.6	5	0.15	0.15	0.999	0.999	0.45	0.89
	0	82.1	-48.7	0.45	0.35	22.3	24.5
	1	42.8	-13.2	0.44	0.17	68.2	81.9
240.2	2	35.5	-3.5	0.54	0.17	98.7	136
	3	18.5	6.4	0.72	0.45	93.8	157
	4	5.4	4.6	0.93	0.84	34.4	75.7
162.6	5	1.1	1.2	0.99	0.98	7.1	13.9
	6	0.20	0.21	0.998	0.998	1.1	1.7
	7	0.03	0.03	1.00	1.00	0.16	0.18
240.2	0	97.4	-60.8	0.31	0.12	16.0	17.4
	1	104.4	-40.5	0.14	0.09	52.1	52.6
	2	67.4	-31.5	0.07	0.12	88.1	87.0
162.6	3	24.4	-11.2	0.15	0.24	121.3	116.6
	4	10.9	1.5	0.49	0.50	121.7	120.0
	5	4.7	3.02	0.82	0.80	63.3	21.2
240.2	6	1.45	1.26	0.96	0.95	18.7	4.64
	7	0.36	0.34	0.99	0.99	4.23	0.83
	8	0.08	0.08	0.999	0.999	0.84	0.12
162.6	0	-62.8	-78.3	0.19	0.30	9.9	9.4
	1	-56.3	-66.0	0.24	0.33	29.1	27.6
	2	-48.2	-56.3	0.26	0.38	48.0	44.1
240.2	3	-37.1	-41.0	0.31	0.44	65.4	58.1
	4	-22.9	-25.1	0.38	0.50	79.2	69.6
	5	-10.1	-11.9	0.52	0.60	82.5	72.6
162.6	6	-2.7	-3.8	0.71	0.74	66.0	59.8
	7	-0.26	-0.63	0.87	0.88	37.5	35.6
	8	0.16	0.09	0.95	0.95	16.0	15.7
240.2	9	0.12	0.11	0.99	0.99	5.7	5.6
	10	0.05	0.06	0.996	0.996	1.8	1.8

TABLE III. Values of the real and imaginary parts of forward scattering amplitudes. $\mathcal{F}_N(0)$ is calculated in the absence of the Coulomb interaction and $f_N(0)$ is defined as, $f_N(0) = \sum_l (2l+1) \exp(2i\sigma_l) (\eta_l \exp(2i\delta_l) - 1) / 2ik_0$.

T_π (MeV)	k_0 (fm ⁻¹)	$\mathcal{F}_N(0)$ (fm)		$f_N(0)$ (fm)					
		(a)	(b)	(a)	(b)				
40 (π^+)	0.5659	1.35 + i	0.37	1.16 + i	1.15	1.30 + i	0.51	1.07	+ i 1.21
49.7 (π^+)	0.6421	2.03 + i	0.62	1.66 + i	1.64	1.92 + i	0.83	1.48	+ i 1.71
79.3 (π^+)	0.8435	4.30 + i	2.74	2.05 + i	3.91	3.88 + i	3.10	1.65	+ i 3.97
114.3 (π^+)	1.058	4.55 + i	6.00	0.84 + i	6.72	3.66 + i	6.44	0.0089	+ i 6.58
162.6 (π^+)	1.332	1.96 + i	9.31	0.14 + i	8.42	0.47 + i	9.27	-1.08	+ i 8.12
240.2 (π^+)	1.745	-2.67 + i	10.50	-3.74 + i	10.41	-4.33 + i	9.42	-5.32	+ i 9.14
342.6 (π^+)	2.267	-6.00 + i	8.94	-6.45 + i	9.64	-7.13 + i	7.02	-7.71	+ i 7.61
114.3 (π^-)	1.058	4.55 + i	6.00	0.61 + i	6.75	5.39 + i	5.37	1.50	+ i 6.76
162.6 (π^-)	1.332	1.96 + i	9.31	-0.15 + i	8.63	3.49 + i	9.04	1.20	+ i 8.75

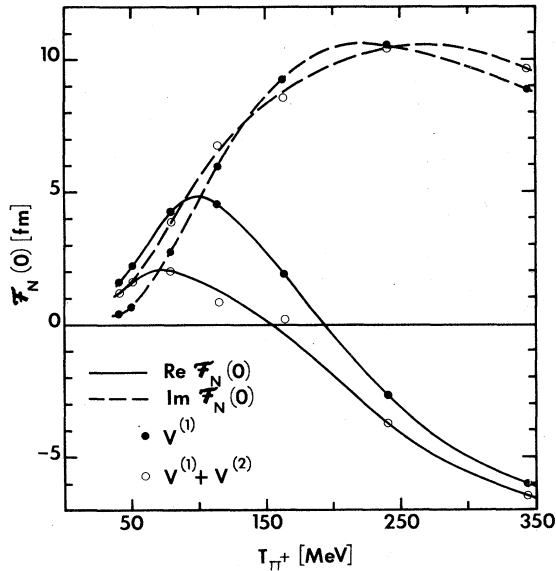


FIG. 6. Values of the real and imaginary parts of the nuclear scattering amplitude $\mathcal{F}_N(0)$ calculated in the absence of the Coulomb interaction. The amplitudes shown are those calculated with $V^{(1)}$ only and those calculated with $V^{(1)} + V^{(2)}$. (See Table III.)

III. CONCLUSIONS

As we have seen, the inclusion of a second-order optical potential leads to excellent fits to the data for pion-nucleus scattering. There is a significant effect on the differential cross sections at all energies, however, the modifications in the cross sections are largest at low energies, where the first-order potential is quite small. (As we have noted in Sec. II, the calculation of the low-energy first-order optical potential requires some improvement.)

We believe that our careful calculation of the first-order potential has enabled us to provide a meaningful parametrization of the second-order potential. The fact that the parameters for π - ^{12}C and π - ^{16}O scattering are similar is encouraging, however, further tests of our optical model are called for. The use of the pion optical wave functions calculated using our potential in the description of various inelastic processes would be of value.

This work was supported in part by the National Science Foundation and the PSC-BHE Research Program of the City University of New York.

¹L. C. Liu and C. M. Shakin, Phys. Rev. C **16**, 333 (1977).

²R. H. Landau, S. C. Phatak, and F. Tabakin, Ann. Phys. (N.Y.) **78**, 299 (1973); R. H. Landau, Phys. Rev. C **15**, 2127 (1977) and the references listed therein.

³R. H. Landau and A. W. Thomas, Phys. Lett. **61B**, 361 (1976); L. C. Liu and C. M. Shakin, Phys. Rev. C **16**, 1963 (1977).

⁴L. C. Liu, Phys. Rev. C **17**, 1787 (1978).

⁵L. Celenza, L. C. Liu, and C. M. Shakin, Phys. Rev. C **11**, 1593 (1975); (E) **12**, 721 (1975).

⁶D. J. Malbrough *et al.*, LASL Report No. LA-UR-77-1939 (unpublished).

⁷J. P. Albanese, J. Arvieux, E. Boschitz, C. H. Q. Ingram, L. Pflug, C. Wiedner, and J. Zichy, Phys. Lett. **73B**, 119 (1978); E. Boschitz, private communications.

⁸J. T. Londergan, K. W. McVoy, and E. J. Moniz, Ann. Phys. (N.Y.) **86**, 147 (1974).

⁹R. H. Landau and A. W. Thomas, Nucl. Phys. (to be published).

¹⁰L. C. Liu and C. M. Shakin, Phys. Rev. C **18**, 604 (1978).